TU Delft

Challenging Glass 3 – Conference on Architectural and Structural Applications of Glass,
Bos, Louter, Nijsse, Veer (Eds.), TU Delft, June 2012.

Experimental and Numerical Analysis of Edge Seal Spacers of Insulated Glass Units for Structural Sealant Glazing Applications

Anneliese Hagl
A. Hagl Ing. GmbH, Germany, www.a-hagl-ingenieure.de

For applications beyond the European Technical Guideline ETAG 002 for structural sealant glazing (SSG), a detailed knowledge of the mechanical characteristics of all components is required. While the physical properties of glass, steel and aluminum and silicone adhesives are quite well known or in the focus of current research activities, edge seal spacers of insulated glass units have not been investigated yet in detail. Edge seal spacers show a high level of design variations and thus their behavior differ significantly with respect to the various designs. This paper focuses on experimental results of compressive tests of edge seal spacers which build the basis for the derivation of numerical models allowing to analyze SSG designs and applications beyond ETAG 002.

Keywords: Edge Seal, ETAG 002, Insulated Glass, Spacer, SSG,

1. Introduction

Usually, structural sealant glazing (SSG) designs are covered by the European guideline ETAG 002 [1]. As the bond between glass and supporting structure shows complex mechanical performance characteristics, simplifying assumptions are derived for sizing neglecting also the characteristics of the edge seals and their impact on insulating glass units. Thus a detailed knowledge of bond and edge seal material behavior is not required. Nevertheless, progress demonstrated that in-detail studies lead to improved physical insight which might be important for applications beyond ETAG 002 as for example cold bending applications [2].

In order to extend numerical procedures to insulated glass units the adequate modeling treatment of structural edge seals is of major importance. Edge seals ensure the air tightness of the insulating glass under operating conditions and provide spacing between the glass panes. Spacers are the core components of edge seals differing significantly in layout. The design of the spacers might be based either on metals or polymers or on combinations enclosed by butyl strips. Regarding metallic designs, stainless steel or aluminum are first choices for material. For polymers, additional distinction is made between foam and homogenous material. Thus, mechanical properties of the spacers are expected to differ significantly.

As first step towards understanding of edge seal behavior, compressive tests were performed of spacer specimens of various designs. The baseline specimens consist usually of pieces of approximately 50 mm length. This paper presents experimental

results showing significant differences in the structural performance of the various designs. Detailed finite element studies of the tests were performed in order to check for applicability of numerical procedures for predictive capabilities of structural edge seals. Beyond the experimental results, focus in the paper is put on the derivation of simplified mechanical models for application on global structural SSG models. Outlook of these research activities is to improve SSG sizing towards higher loads taking into account edge seal behavior.

2. Insulated Glass Units and Edge Seal Spacers

Insulated glass units consist of two or more glass panes with the volume(s) between the panes filled by air or gas in order to decrease thermal conductivity for improved insulation properties. In addition to the glass panes the insulated glass units are composed of a combination of edge seals and edge seal spacers for mechanical integrity with the edge seals typically based on silicone adhesives and the spacers as dedicated sub-components, see Figure 1. This combination acts in parallel as sketched in Figure 2 when the insulating glass units are exposed to wind loads or similar. The stiffness properties of both glass panes and spacers determine the load share between spacers and edge seal. Other load cases especially related to insulating glass units are climate loads due to the expansion of the insulating fluid between the panes in case of temperature increase and installation loads due to different atmospheric conditions (pressure altitudes) between manufacturing site and installation site. The following table presents the characteristics of the edge seal loading for these load cases assuming constant pressures (isobaric case) or constant volumes (isochoric case) of the insulating fluid as extreme cases:

Table 1: Insulating glass unit load cases.

Specimen	Insulating fluid volume (isobaric case)	Insulating fluid pressure (isochoric case)	Resulting edge seal loading
High temperature	Increasing volume	Increasing pressure	Tensile loading
Low temperature	Decreasing volume	Decreasing pressure	Compression loading
High pressure altitude	Increasing volume	No change	Tensile loading
Low pressure altitude	Decreasing volume	No change	Compression loading

While the isobaric case is related to infinitely flexible glass units, the isochoric case represents infinitely stiff glass units. Due to flexibility of the glass panes and the other insulating glass components neither the pure isobaric case not the isochoric case are expected in reality. Instead a combination of volume and pressure changes will occur.

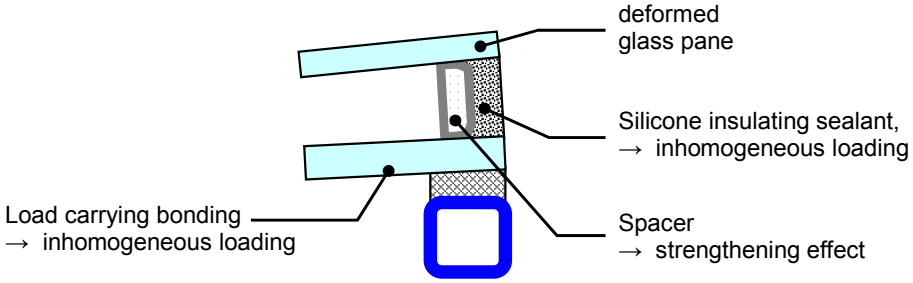

Figure 1 : Sketch of insulated glass unit used in SSG design [2].

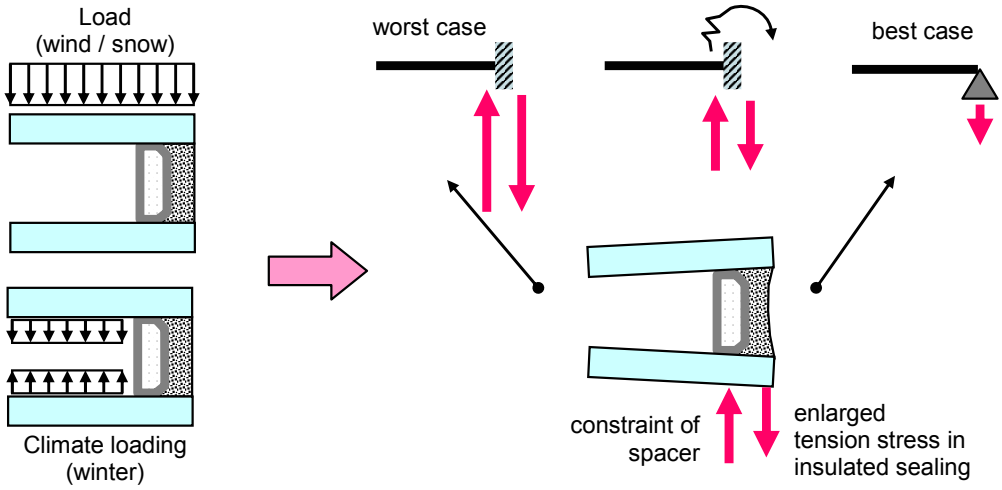

Figure 2 : Load schemes of edge seals of insulated glass units.

Edge seal spacers are used in insulating glass units to fix the distance between the glass panes of the unit. Typically the spacers are composed of a body consisting of either metals or polymers or combinations of both plus adhesive strips on each contact surface of the glass panes based on butyl material. Figure 3 presents typical edge seal spacer designs while Figure 4 shows the functional environment of an edge seal spacer.

Figure 3 : Edge seal spacer designs: Left side visible inside insulating glass unit.

The spacer is attached to the glass panes by an inner seal made of butyl material. Depending on the spacer design the butyl has to be added to the spacer or is directly integrated. Thus loads transferred from the glass panes to the spacers have to pass the butyl strips. E.g. for compressive or tensile loads, the edge seal spacer assembly can be mechanically interpreted as three flexible elements put in series. Thus the effective stiffness of the edge seal spacer assembly can be approximated by calculating the harmonic mean of the butyl and spacer stiffness values.

While design procedures are available for the edge sealant in case of SSG designs by the guideline ETAG 002, the impact of the spacer assembly on the global mechanical behavior is typically neglected in design codes. Furthermore, although detailed thermal analysis can be found in the advertisements of the manufacturers for advanced spacer designs related mechanical properties are never indicated. Therefore, several spacer designs were experimentally investigated in order to get an overview of the mechanical behavior of these components.

3. Experimental Activities

3.1. General Approach

Load cases of interest for the edge seal spacers are tensile and compressive loading and shear loading. Regarding these load cases, the compressive load case is selected as most interesting one as – comparing to the tensile load case – no adhesive failure is expected and compared to the shear load case, tensile and compressive load cases are assumed to be more complex in their mechanical behavior. In order to reduce buckling two test articles are combined into one specimen as shown in Figure 5. Please note that in the insulating glass unit application case the edge seal spacer is stabilized by the edge sealant.

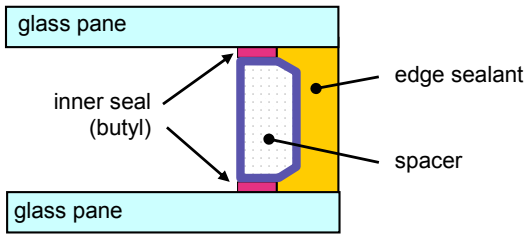

Figure 4 : Elements of edge seal spacers.

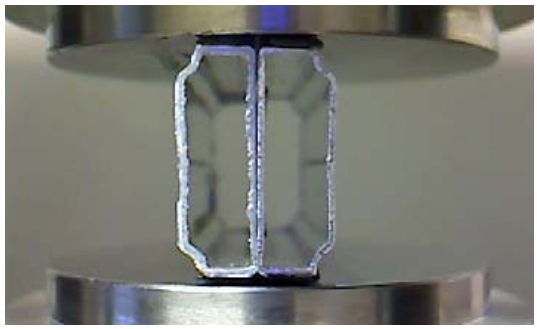

Figure 5 : Test set-up for edge seal spacer testing.

Beyond understanding of the spacer behavior and insight into deformation patterns, quantitative objective of the test campaign is the derivation of stiffness parameters for the various spacer designs. In this first exploration phase monotonous load histories were applied. Based on experience of the first test campaign more complex load histories will be designed e.g. in view of tensile loading and of cyclic loading.

3.2. Component Testing: Butyl Strips

While the linear-elastic material description of metallic parts such as aluminum and steel is straight forward using well-known values for the Young's modulus and the Poisson's ratio, the adequate description of the material behavior of the butyl strip is less obvious. Therefore, butyl strips of 3.5 mm width were separately tested under compressive loads on 50 mm strip length in a similar manner as the edge seal spacers. Figure 6 presents the results in terms of loads versus displacements. The curve shows a progressive behavior i.e. stiffness increases with loads. While for low loads, the stiffness will probably be mainly related to the butyl strip, for very high loading and thus very high stiffness, the flexibility of the test set-up has to be considered for

quantitative evaluation as well. After unloading and inspecting the specimen, it can be seen that the butyl strip deforms mainly in a plastic manner.

As first step the material characteristics obtained by the load curve are mapped into elastic material laws – either linear or hyperelastic. This kind of black box approach – relating displacement inputs to load outputs – is adequate as long as the load scheme – compressive monotonous loading – is not changed. Future steps might result in the application of plastic or elasto-plastic material laws for the Butyl strips. For the current numerical studies, it is assumed that the deformation range of the Butyl strips do not exceed a range of 5% - 10% engineering strain. Thus the material laws for the Butyl strip were adjusted within these intervals.

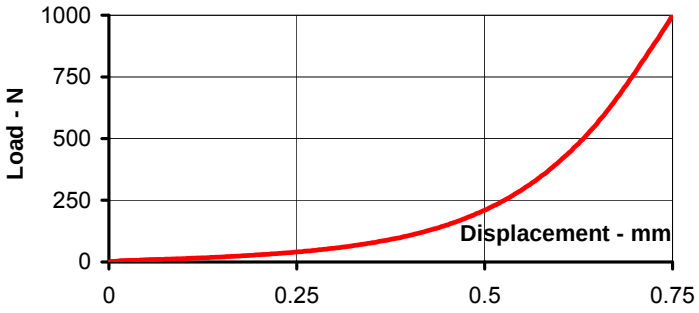

Figure 6 : Experimental results of butyl strip testing.

3.3. Testing of D-shape Aluminum Edge Seal Spacers

Next, the various edge seal spacers were tested in a similar manner. Figure 7 shows the design of the first test series featuring D-shaped aluminum bodies of three different heights. The specimens were delivered without butyl strip and with heights of 13.5 mm (labeled small size in the paper), 15.5 mm (labeled mid size in the paper) and 17.5 mm (labeled large size in the paper). It is assumed that the nominal spacing amounts to 14 mm, 16 mm and 18 mm respectively leading to nominal butyl strip thickness values of 0.5 mm in total for both ends. The butyl strips used for the derivation of material laws showed a thickness of approximately 0.9 mm. These strips were also applied to the D-shape spacers within this test campaign.

Figure 7 : D-shape aluminum spacers. of heights 13.5 mm, 15.5 mm, 17.5 mm

Figure 8 presents the mechanical characteristics of the D-shape aluminum spacers. The figure left shows the distributed loads, i.e. the loads per length spacer, for a representative specimen. The decrease of loads for large displacements is due to a kind

of buckling. It is expected that the real loading range is significantly below this load peak. Therefore, results for the three designs are presented in the figure right. The following statements can be drawn from this figure: First the results rank in highest stiffness for the mid spacer size, immediately followed by the small spacer size and finally the large spacer design with significantly lower levels. This is slightly inconsistent to what is expected at first glance from theory. As the smallest spacer theoretically features the highest stiffness, the expected ranking is small spacer – mid spacer – large spacer.

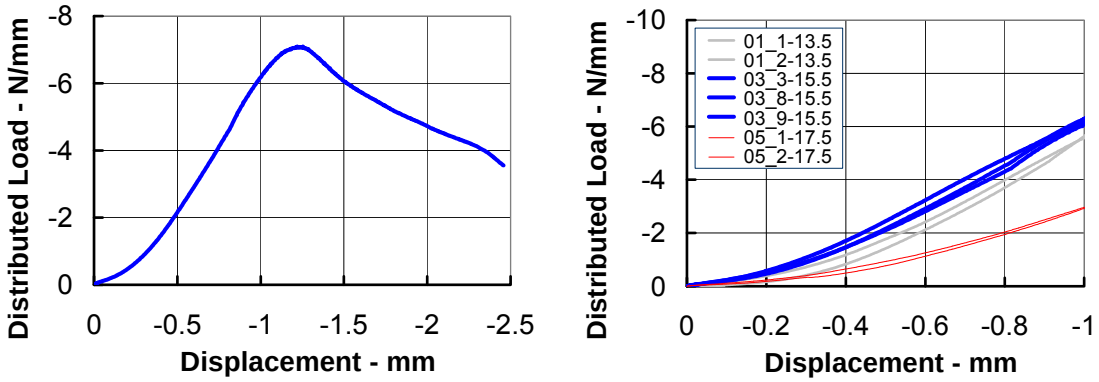

Figure 8: Mechanical characteristics of D-shape aluminum spacers.

3.4. Testing of D-shape Steel Edge Seal Spacers

In accordance to the Aluminum spacers the D-shape steel spacers were tested and evaluated in a similar manner. While Figure 9 shows a photograph of these spacers, Figure 10 presents the experimental results in terms of load curves. The steel spacers are slightly stiffer compared to the aluminum spacers and again dependency on size is not consistent with expectations from a theoretical point of view.

Figure 9: D-shape steel spacers of heights 13.5 mm, 17.5 mm, 15.5 mm

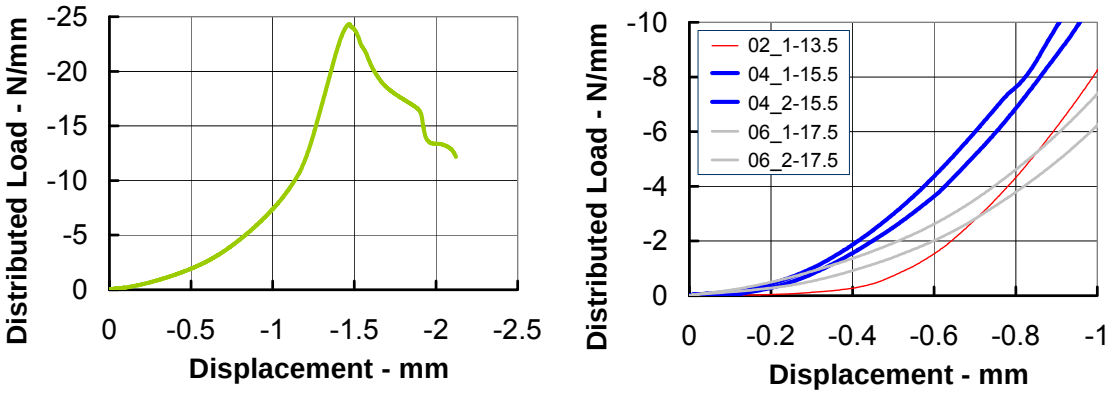

Figure 10: Mechanical characteristics of D-shape aluminum spacers.

3.5. Testing of Composed Edge Seal Spacers

Spacers composed of polymer and metallic parts are gaining more interest in view of low thermal conductivity where pure metallic designs show dis-advantages due to the high thermal conductivity especially of aluminum. Figure 11 presents such a spacer design for low conductivity composed of a polymer body and a steel surface sheet for same heights as before. Figure 12 displays the related load curves leading to the conclusion that the order of magnitude is similar to the pure metallic spacer designs. Again, slight inconsistencies are visible with respect to the ranking of the stiffness characteristics versus spacer size.

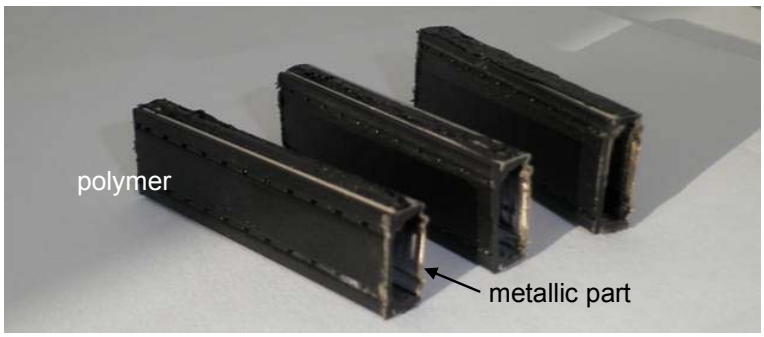

Figure 11: Two-material spacers of heights 13.5 mm, 15.5 mm, 17.5 mm.

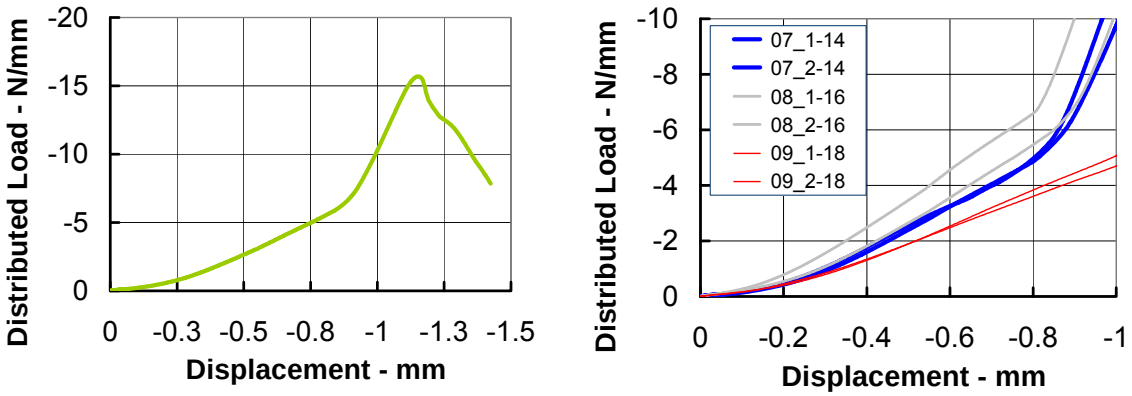

Figure 12: Mechanical characteristics of two-material spacers.

3.6. Comparison of Edge Seal Spacers 15.5mm Height

In order to check for design varieties, edge seal spacers of different shapes from other manufacturers were tested as well. Figure 13 presents C-shape steel spacers, T-shape aluminum spacers and a D-shape spacer composed of polymer and steel for a spacer height of 15.5 mm. In Figure 14 results of 15.5 mm height spacers of steel (C-shape, label S), aluminum (T-shape, label A) and the two-material D-shape spacer (label Co) are presented. It can be seen that with respect to steel and aluminum spacers, the stiffness is lower compared to the spacers presented in the sections before. Nevertheless, the order of magnitude is the same. Regarding a comparison with the D-shape two-material spacer, the mechanical characteristics are quite similar although the Young's modulus of the materials differs significantly.

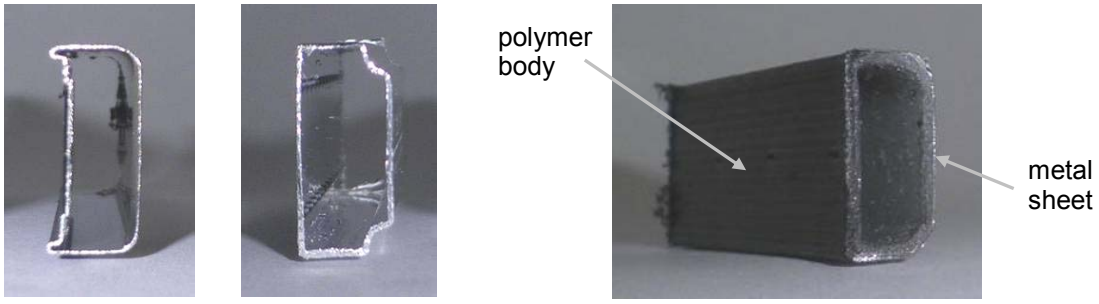

Figure 13 : C-shape steel spacer, T-shape aluminum spacer, D-shape two-part spacer design.

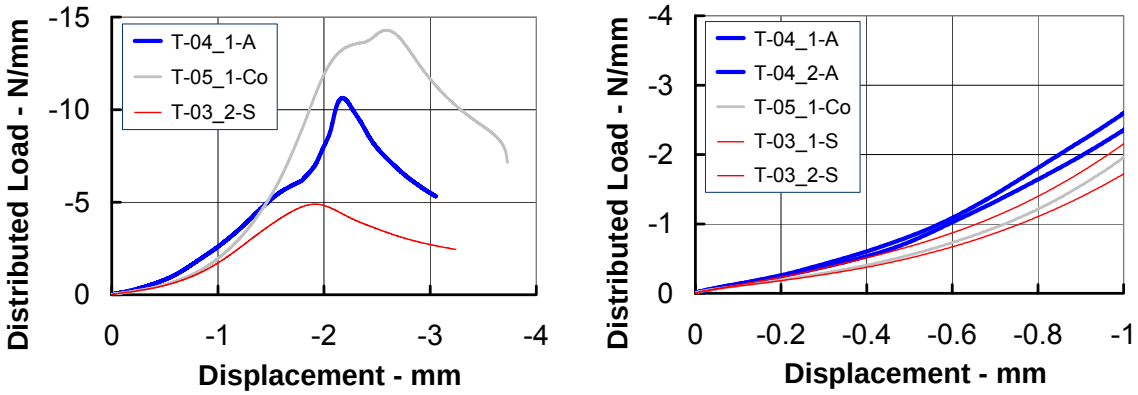

Figure 14: Mechanical characteristics of different spacer designs of 15.5mm height

4. Numerical Results

4.1. Finite Element Analysis of Butyl Strip

First, a material law for butyl needs to be derived from the butyl strip measurements mentioned above. In this phase, a simple isotropic linear-elastic material law was selected in order to get an overview of the mechanical behavior. For the calculation of a representative stiffness value for butyl, a load curve gradient was calculated based on collocation points at 5% and 10% engineering strain levels leading to a stiffness of approximately 2 N/mm per mm strip. A finite element model of the butyl strip was set up and the related material law was adjusted in such a way that the stiffness of the model coincides with that of the test. For the material law Poisson's ratio is required in addition to the Young's modulus which will be accordingly adjusted. The Poisson's ratio was selected close to 0.5 meaning almost incompressible behavior which is typical for hyperelastic material. Regarding the boundary conditions of the finite element model it was assumed that the butyl specimen perfectly sticks to the fittings of the testing machine. This approach is clearly motivated by the sticky behavior of the strips when manipulated.

It is obvious that the selection of a linear material law is only a rough approximation for getting first insight. During unloading of the specimens at the end of the tests, the flattened butyl was totally destroyed and did not significantly recover the original shape. Thus, the material shows an inelastic behavior to a high level. From a numerical point of view further improvement might be the application of an elasto-plastic material law. Regarding testing and subsequent correlations, cyclic tests on the one hand and other

load schemes such as cyclic, tensile or shear tests of the butyl strips are of high interest for future exploration.

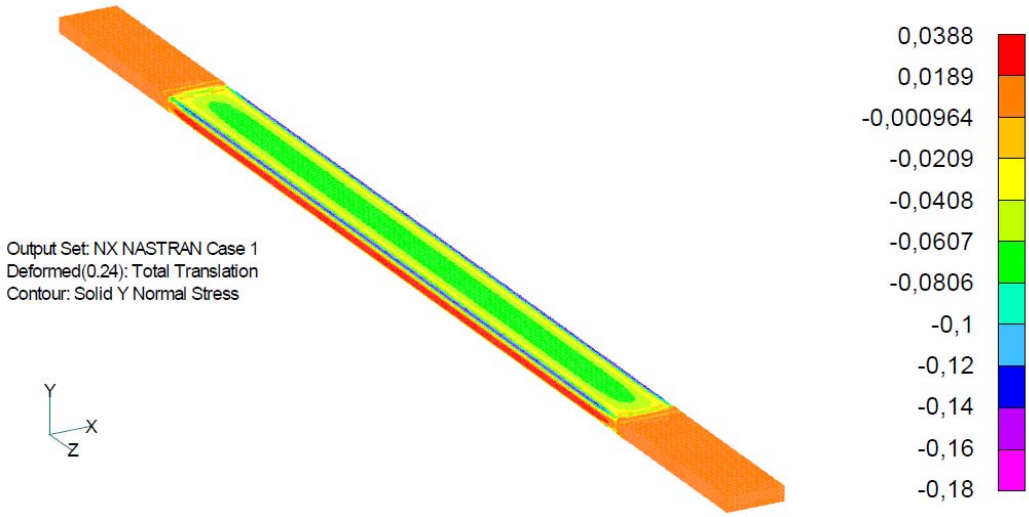

Figure 15 : Finite element analysis of butyl strip presenting normal stress distributions.

4.2. Finite Element Analysis of Nominal D-shape Spacers

Both 3D and 2D linear finite element analysis were performed for the D-shape aluminum and steel spacers including butyl strips of nominal thickness of 0.25 mm on each side. The spacers were modeled by shell elements while the butyl is treated by solids as done in the section before. The comparison between 2D and 3D analytical models allows to judge edge effects. The comparison between aluminum and steel will the drawing of conclusions with respect to the material. The following table presents the stiffness values derived from the finite element analysis. Please note that high uncertainty is related to geometry. The aluminum spacers are assumed to feature a thickness of 0.4 mm while for steel spacers, the thickness seems to be lower. For comparison, thickness values of 0.4 mm and 0.3 mm are presented here. The stiffness refers to a strip of 1 mm width leading to a unit of N/mm^2.

Table 2: Numerical stiffness values for D-shape spacers.

Spacer design Material – height - thickness	Stiffness 3D model N/mm^2	Stiffness 2D model N/mm^2	Difference %
Aluminum 13.5 mm, 0.4 mm	15.74	16.08	2.14
Aluminum 15.5 mm, 0.4 mm	15.63	15.97	2.13
Aluminum 17.5 mm, 0.4 mm	15.54	15.87	2.13
Steel 13.5 mm, 0.4 mm	17.66	18.07	2.32
Steel 15.5 mm, 0.4 mm	17.61	18.02	2.32
Steel 17.5 mm, 0.4 mm	17.58	17.98	2.32
Steel 13.5 mm, 0.3 mm	15.93	16.54	3.80
Steel 15.5 mm, 0.3 mm	15.84	16.44	3.79
Steel 17.5 mm, 0.3 mm	15.76	16.36	3.77

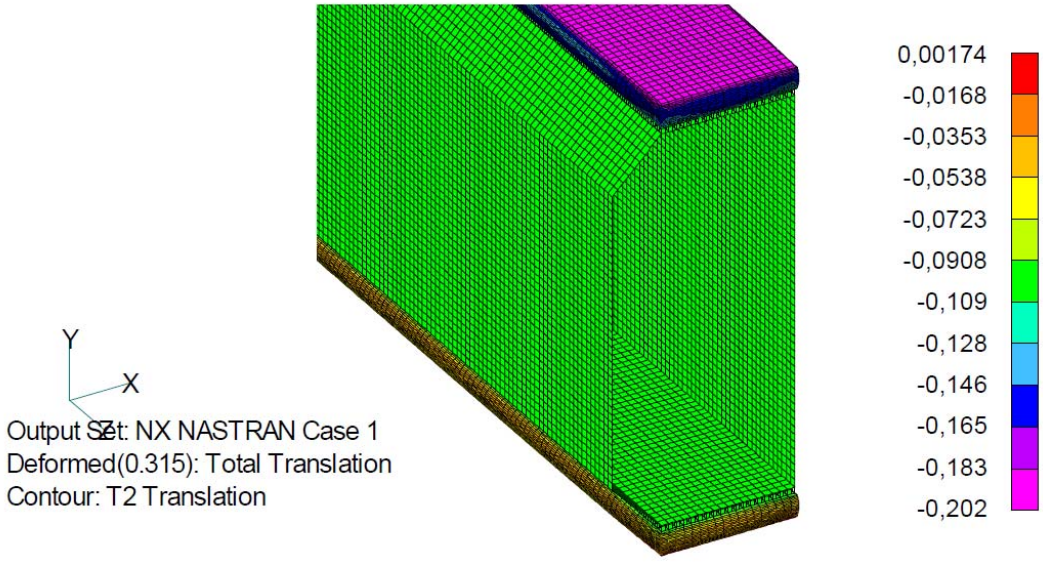

Figure 16 : Finite element analysis of D-shape spacer indicating large compressive strains in the butyl strips.

The results of the tables allows for the following conclusions:

- Edge effects are negligible as the differences between 3D and 2D finite element models are quite small.
- The spacer stiffness is not a key parameter as seen by the comparison between aluminum and steel (Young's modulus ratio approx. 3!) and by the comparison of different thicknesses for steel.
- Nevertheless the trends in the differences are consistent with theory i.e. steel of same thickness behaves stiffer than aluminum and thickness 0.4 mm behaves stiffer than 0.3 mm.
- Obviously the butyl strips are the key in the mechanical behavior showing high flexibility.

4.3. Comparison with Experimental Data

In a next step, the results were compared to the experimental values. It is obvious that the numerical stiffness results presented in the section before are significantly higher than the experimental ones. As the butyl strip was identified as key element for the mechanical behavior a closer look was put on the butyl modeling. It was already mentioned before that the butyl strips are applied for the test campaign based on 0.9 mm thick strips. Thus, the tested spacer elements featured higher thickness for the butyl strips than assumed for the finite element models leading to a lower stiffness of the assembly. Therefore, calculations were performed with modified models featuring 0.9 mm thickness at each interface. Table 3 presents the results and comparisons with experimental stiffness results based on displacement levels of 0.09 mm and 0.18 mm (corresponding to 5% and 10% with respect to an assumed butyl thickness of 0.9 mm).
First, it should be mentioned that the experimental stiffness values are expected to highly depend on pre-loading of the specimens. The number of test results for evaluation is given in brackets. For a more quantitative approach it is evident that more specimens are required in view of uncertain parameters. Nevertheless clear tendencies are obvious. The experimental stiffness levels are typically bracketed by the numerical results with larger butyl width on the lower side and with smaller butyl widths on the upper side.

Table 3: Comparison of 2D stiffness values with experimental results for D-shape spacers.

Spacer design Material – height - thickness	Test N/mm^2	0.25 mm butyl N/mm^2	0.9 mm butyl N/mm^2
Aluminum 13.5 mm	2.13 (1)	16.08	1.67
Aluminum 15.5 mm	2.65 (6)	15.97	1.67
Aluminum 17.5 mm	1.17 (1)	15.87	1.67
Steel 13.5 mm	2.86 (2)	16.54	1.68
Steel 15.5 mm	2.41 (2)	16.44	1.68
Steel 17.5 mm	2.73 (2)	16.36	1.68

5. Simplified Models

For global numerical models of insulating glass units e.g. in the context of comprehensive SSG façade analysis, reduced order models are desirable for representation of edge seal spacer characteristics. Thus, this section is dedicated to the challenge to represent the edge seal spacer assembly by lumped stiffness parameters e.g. by spring elements. Figure 17 sketches this approach in an illustrative manner.

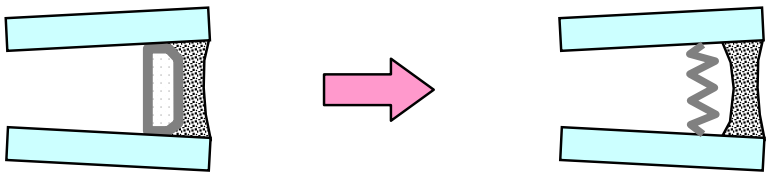

Figure 17 : Simplification of mechanical edge seal spacer model.

For this simplified model, the axis where bending is decoupled from tensile/compressive loading needs to be identified. The axis is obtained by relating the constraint moments to the constraint forces. The following tables present the axis offsets for the D-shape aluminum spacers with respect to the origin on left bottom corner. As it can be seen the spacer height is of second order with respect to the offset value. This finding underlines the dominance of the butyl strips as mentioned in the section before.

Table 4: Key figures of mechanical properties of D-shape edge seal spacers.

Spacer design Material – height - thickness	Offset mm^2	Tensile stiffness N/mm^2	Bending stiffness N/rad
Aluminum 13.5 mm	4.105	16.08	16.77
Aluminum 15.5 mm	4.107	15.97	16.76
Aluminum 17.5 mm	4.108	15.87	16.75

Figure 18 presents a comparison of the numerical results obtained with a detailed model of the edge seal spacer and with a simplified model consisting of a spring element representing the normal and bending stiffness characteristics. The deformation fields presented in Figure 18 confirm the mechanical adequacy of the two models.

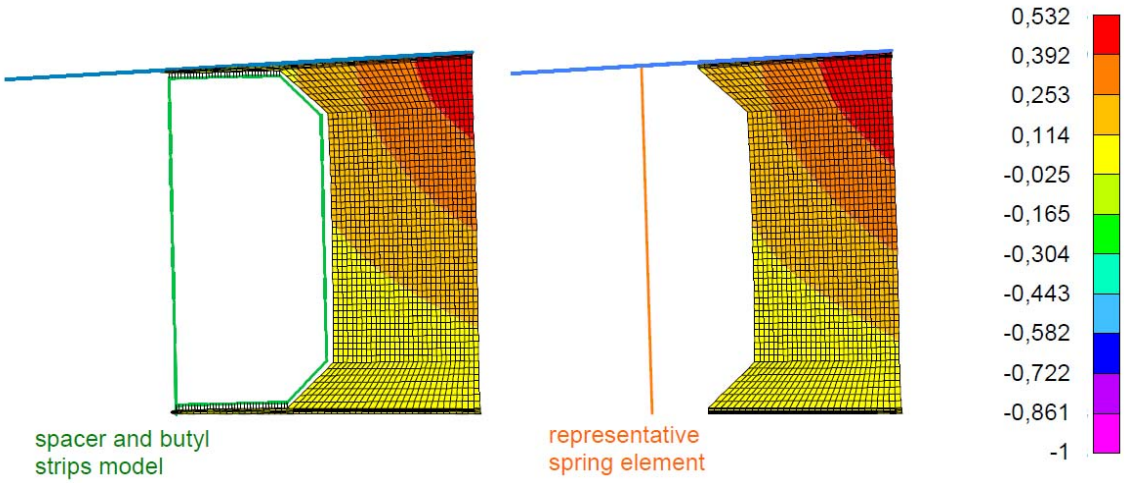

Figure 18 : Comparison of numerical models – left detailed model, right simplified model featuring a representative spring element.

6. Conclusions and Outlook

Edge seal spacer designs were subjected to compressive load schemes by both experiments and numerical studies. The butyl strips were identified to be dominant with respect to the mechanical characteristics of the edge seal spacer assembly. Due to this finding, the geometry of the butyl strips and the related deformations of the butyl during the manufacturing process need more attention in the future for accurate mechanical models.

Within this paper the butyl strips were exposed to monotonous compressive loading. For future studies it is recommended to consider cyclic load histories as well allowing to model the inelastic behavior of the butyl material in more detail. In addition the behavior of the butyl strips shall be investigated with respect to different load schemes such as shear or combined load schemes.

Furthermore, the mechanical characteristics of the edge seal spacer assembly were reduced to a spring element defined by the location of the end grids, the normal and the bending stiffness. This modeling approach showed adequate behavior and can thus be applied to global modeling of insulating glass units of SSG designs for linear finite element analysis.

7. Acknowledgements

For providing samples of the edge seal spacers, the author would like to thank the contributing glass manufacturers – especially the companies Wagener, Roschmann and Okalux. Furthermore Test-Ing Material GmbH [3] is acknowledged for performing the experimental campaign of the edge seal spacers.

8. References

[1] NN; *ETAG 002 Guideline for European Technical Approval for Structural Sealant Glazing System (SSGS) – Part 1 Supported and unsupported systems*, www.eota.be/pdf/ssgs-fin-am3.pdf

[2] Hagl, A., Dieterich, O., *Glass Unit Corner Loading – Key Parameter in Durability*, 4th Symposium on Durability and Construction Sealants and Adhesives, June 2011, Anaheim, CA

[3] www.test-ing-material.de